P38 Initiates Diabetic Neurodegeneration Through Glutamatergic and GABAergic Neurons

Aisan Farhadi
Royan Institute for Stem Cell Biology and Technology
Mehdi Totonchi
Royan Institute for Stem Cell Biology and Technology
Seyed Masood Nabavi
Royan Institute for Stem Cell Biology and Technology
Hossein Baharvand
Royan Institute
Hossein Pakdaman
Shaheed Beheshti University of Medical Sciences
Ensiyeh Hajizadeh-Saffar
Royan Institute for Stem Cell Biology and Technology
Ahmad Mousavi
Royan Institute for Stem Cell Biology and Technology
Fatemeh Hadi
Royan Institute for Stem Cell Biology and Technology
Hamed Al-Sinawi
Durban University of Technology
Quan Li
Wenzhou University
Jin-San Zhang (zhang.jinsan@mayo.edu)
Wenzhou Medical University https://orcid.org/0000-0002-4436-9593
Yaser Tahamtani
Royan Institute for Stem Cell Biology and Technology
Koorosh Shahpasand
Royan Institute for Stem Cell Biology and Technology

Research article

Keywords: Diabetes mellitus, neurodegeneration, P38, tau pathology

Posted Date: July 21st, 2020

DOI: https://doi.org/10.21203/rs.3.rs-41603/v1

P38 Initiates Diabetic Neurodegeneration Through Glutamatergic and GABAergic Neurons

Aisan Farhadi[1,2,3], Mehdi Totonchi[1,4], Seyed Masood Nabavi[3], Hossein Baharvand[1,2,3], Hossein Pakdaman[5], Ensiyeh Hajizadeh-Saffar[6], Ahmad Mousavi[1], Fatemeh Hadi[3], Hamed Al-Sinawi[7], Quan Li[8], Jin-San Zhang[8,9*], Yaser Tahamtani[1,10*], and Koorosh Shahpasand[1,3*]

[1]Department of Stem Cells and Developmental Biology, Cell Science Research Center, Royan Institute for Stem Cell Biology and Technology, ACECR, Tehran, Iran

[2]Department of Developmental Biology, University of Science and Culture, Tehran, Iran

[3]Department of Brain and Cognitive Sciences, Cell Science Research Center, Royan Institute for Stem Cell Biology and Technology, ACECR, Tehran, Iran

[4]Department of Genetics, Reproductive Biomedicine Research Center, Royan Institute for Reproductive Biomedicine, ACECR, Tehran, Iran

[5]Brain Mapping Research Center, Department of Neurology, Shahid Beheshti University of Medical Sciences, Tehran, Iran

[6]Department of Regenerative medicine, Cell Science Research Center, Royan Institute for Stem Cell Biology and Technology, ACECR, Tehran, Iran

[7]Department of Behavioral Medicine, Sultan Qaboos University Hospital, Muscat, Oman.

[8]Institute of Life Sciences, Wenzhou University, Wenzhou, Zhejiang 325035, China

[9]Division of Oncology Research, Mayo Clinic, Rochester, MN 55905, USA

[10]Department of Diabetes, Obesity and Metabolism, Cell Science Research Center, Royan Institute for Stem Cell Biology and Technology, ACECR, Tehran, Iran

[*]Correspondences:

1) K Sh, Department of Brain and Cognitive Sciences, Cell Science Research Center, Royan Institute for Stem Cell Biology and Technology, ACECR, Tehran, Iran. Email: shahpasand@royaninstitute.org

2) Y T, Department of Stem Cells and Developmental Biology, Cell Science Research Center, Royan Institute for Stem Cell Biology and Technology, ACECR, Tehran, Iran. Email: yasertahamtani@royaninstitute.org

3) J.S Z, Division of Oncology Research, Mayo Clinic, Rochester, MN 55905, USA, Email: Zhang.JinSan@mayo.edu

Email addresses of all co-authors:

Author Name	Email address	ORCID ID
Aisan Farhadi	a.farhadi69@yahoo.com	https://orcid.org/0000-0002-2049-7988
Mehdi Totonchi	totonchimehdi@gmail.com	https://orcid.org/0000-0002-7285-3155
Seyed Masood Nabavi	seyedmassoodnabavi@gmail.com	https://orcid.org/0000-0002-9814-8083
Hossein Baharvand	baharvand@royaninstitute.org	http://orcid.org/0000-0001-6528-3687
Hossein Pakdaman	hpakdaman20@gmail.com	https://orcid.org/0000-0001-7054-8854
Ensiyeh Hajizadeh-Saffar	Hajizadeh.ehs@gmail.com	https://orcid.org/0000-0003-4933-5250
Ahmad Mousavi	ahmad.moousavi@gmail.com	http://orcid.org/0000-0003-3845-3286
Fatemeh Hadi	arian_hadi68@yahoo.com	https://orcid.org/0000-0002-1292-8290
Hamed Al-Sinawi	senawi@squ.edu.om	https://orcid.org/0000-0001-6705-8459
Qun Li	2295477106@qq.com	NA
Yaser Tahamtani	yaserta@yahoo.com	https://orcid.org/0000-0003-2360-4985
Koorosh Shahpasand	shahpasand@royaninstitute.org	http://orcid.org/0000-0003-2153-0564
Jin-San Zhang	Zhang.jinsan@mayo.edu	https://orcid.org/0000-0002-4436-9593

Abstract

Background: Diabetes mellitus may cause neurodegeneration, but the exact mechanism by which diabetic conditions induce neuronal cell death remains unclear. Tau protein hyperphosphorylation is considered to be a major pathological hallmark of neurodegeneration and can be triggered by diabetes. Various tau-directed kinases, including P38, can be activated upon diabetic stress and induce tau hyperphosphorylation. Despite extensive research efforts and the known importance of tau pathology in neurodegeneration, the exact tau specie(s) and kinases driving neurodegeneration in diabetes mellitus have not been clearly elucidated.

Methods: We herein employed protein expression data analysis as well as immunofluorescence and immunoblotting techniques to determine the exact molecular mechanism of tau pathology triggered by diabetes in both *in vitro* and *in vivo* systems.

Results: We found that P38, a major tau kinase, was increased in Glutamatergic & GABAergic neuron subtypes under diabetic conditions. This rendered them more responsive to oxidative stress caused by diabetes. We observed that oxidative stress activated P38, which in turn directly and indirectly drove tau pathology in the brainstem (enriched by Glutamatergic & GABAergic neurons), which gradually spread to neighboring brain areas. Notably, P38 inhibition suppressed tau pathogenicity and neurodegeneration in diabetic mouse models.

Conclusion: The data establish P38 as a central mediator of diabetes mellitus induced tau pathology. Furthermore, the inhibition of P38 at early stages of diabetes-induced stress can inhibit tau pathology. Our findings provide mechanistic insight on the consequences of this metabolic disorder on the nervous system.

Key words: Diabetes mellitus; neurodegeneration; P38; tau pathology

Background

Diabetes mellitus (DM) is the most common and costly metabolic disorder and can lead to different complications affecting multiple organs, including the CNS [1]. An increasing number of epidemiological, clinical and neuroimaging studies have shown that type 1 or 2 diabetes (T1D, T2D) is an important cause of neurodegeneration [2-5]. It has been reported that DM can be associated with brain atrophy and ultrastructural changes in the white matter, hippocampus, as well as the cortex [6-8]. Some studies have shown that DM can cause neurodegeneration through tau protein hyperphosphorylation and formation of neurofibrillary tangles [9-11]. Elevated levels of hyperphosphorylated tau are frequently detected in the cerebrospinal fluid of diabetes patients compared to those of healthy subjects, irrespective of neurodegenerative disorders [7, 12]. Furthermore, there is tau hyperphosphorylation in both T1D and T2D mouse models [13, 14]. Therefore, it seems that the DM drives tau pathology in the CNS.

Tau is moderately phosphorylated under physiological conditions, whereas tau hyperphosphorylation reflects its pathogenicity and causes neurodegeneration [15, 16]. Hyperphosphorylation of tau leads to its dissociation from microtubules where it then forms aggregates, resulting in neurofibrillary tangles [17]. Of particular importance is that tau phosphorylation in the microtubule-binding sites can reduce its microtubule-binding affinity [18].

Several mechanisms have been proposed to explain how diabetic conditions, such as abnormal insulin signaling pathways and impaired glucose metabolism, which may cause deregulation of tau kinases and phosphatases leading to tau hyperphosphorylation [19-21]. Additionally, DM pathogenic cascades increase oxidative stress and inflammation which can induce tau abnormalities [21]. Glucose deprivation can also induce tau hyperphosphorylation and neurodegeneration; likely through P38 kinase activation [22]. Furthermore,

hyperglycemia can induce oxidative stress, resulting in P38 activation and tau hyperphosphorylation [11]. Apparently, DM dependent stress may activate various tau kinases [23]. Nonetheless, how DM conditions result in comprehensive tau pathology and neurodegeneration remains unclear.

Recently, it has been demonstrated that phosphorylated tau at Thr231 may result in two distinct *cis* or *trans* conformations, a conversion mainly controlled by peptidyl-prolyl *cis-trans* isomerase Pin1 [24]. Pin1 suppression induces *cis* P-tau accumulation [24, 25]. It has been proposed that *cis* P-tau is highly neurotoxic and is an early driver of the tau pathology process upon traumatic brain injury (TBI), chronic traumatic encephalopathy, Alzheimer's disease, and bipolar disorder [24, 26-28]. It has been demonstrated that various stresses, such as: hypoxia or nutritional starvation, suppress Pin1 in various manners, whereby induce *cis* P-tau in cultured neurons [27].

We employed various tau pathology markers including *cis* P-tau as an early driver of tau pathology, AT8 as pretangle detecting antibody and AT180 to investigate tau abnormality processes in DM. We demonstrated that P38 triggered *cis* P-tau accumulation, which spread to other brain areas; reflecting global tau pathology and neurodegeneration under DM conditions.

Material and Methods

Antibodies

The anti *cis* pThr231-tau and anti oxi-Pin1 mouse monoclonal antibodies were from KP Lu, Harvard [25, 27]. The other commercial antibodies were anti-CHAT pAbs (Chemichon,AB5964), anti-TH pAbs (Novus Biologicals,NB100-80063), anti-Vglut1 pAbs (Sigma), anti-GAD65/67 pAbs (Sigma,G5163), anti-IR pAbs (Abcam,ab5500), anti-glucose transporters 2 (Glut2) pAbs (Abcam,ab54460), anti-Glut3 pAbs (Abcam,ab41525), anti-Glut4

pAbs (Abcam,ab654), anti-β-actin mAb (proteintech,IG-60008-1), anti-Pin1 mAb (Santacruz, sc-46660), anti-AT8 P-tau mAb (invitrogen, MN1020), anti-AT180 P-tau mAb (invitrogen, MN1040), Alexa Fluor 488 and 546 secondary antibodies (Abcam,A10036,A-21202,A10040, A-11008).

Primary cortical neuron culture

Primary cortical neurons were isolated from the 17-day-old embryonic (E17) mouse cerebral cortex. Cortical tissue was dissociated with a digestion solution that contained trypsin (Gibco), DNase I (Sigma-Aldrich), HEPES (Sigma-Aldrich), and D-glucose (DG) (Sigma-Aldrich). Isolated neurons were seeded on pre-coated culture dishes with poly-L-ornithine (Sigma-Aldrich) and laminin (Sigma-Aldrich). Isolated cells were cultured with neurobasal medium supplemented with glutamax (Gibco), B27-vitamin A (Gibco), and penicillin-streptomycin (Gibco). After one-day penicillin-streptomycin was removed from the medium.

Hyperglycemia induction in primary cultured neurons

2-Deoxy-D-glucose (2DG) (Sigma-Aldrich) and DG were used to induce hyperglycemia in cultured neurons. Primary neurons were treated with 50 mM 2DG for 24-96 hours. Moreover, primary cultured neurons were treated with 10 mM, 20 mM, 30 mM DG for 2-6 days. They were then harvested for further immunostaining analysis.

Live and dead cell assay

Fluorescein diacetate (FDA) and Propidium Iodide (PI) double staining were used for cell viability assessment. Aliquots of 20 ul of FDA stock solution and 50 ul of PI stock solution were diluted in 10 ml PBS [29]. The cells were initially washed with cold PBS and then the FDA/PI solution was added to the cells and was inspected by a fluorescent microscope after 5 min incubation in room temperature with the solution.

Animal modeling and treatment

Following Royan Institute Ethics Committee approval, the mice were initially divided into healthy (n=5) and Alloxan-induced diabetes (n=5) (NMRI, provided from animal core facility of Royan institute). T1D modeling was carried out with 70 mg/kg single dose Alloxan (Sigma-Aldrich) injection into 8 weeks old male mice. After 4-6 hours fasting, freshly dissolved Alloxan in a buffer (0.9 % NaCl and 1mM HCl) was injected into the mice via the tail vein. After 6 hours fasting, one drop of tail blood was used for fasting blood glucose (FBS) level assessment with a glucometer (Accu-chek active, Germany). Diabetes was confirmed with two repeated blood glucose measurements above than 250 mg/dl. We kept the animals up to 60 days after the injection. All animal protocols were in accordance with the Royan Institute Review Board and Ethics Committee guidelines. Mice were treated with intraperitoneal (IP) 1mg/kg SB203580 (SB) injection for 96 hours.

IP Glucose tolerance test

IP glucose tolerance test (IP-GTT) was performed upon 2g/kg DG injection. We measured the FBS 15, 30, 60, and 90 minutes after IP DG injection.

Immunostaining

For immunostaining analysis, fixed cells were permeabilized (TritonX 0.5%) for 10 min at room temperature. In order to eliminate non-specific primary antibody binding, fixed cells were blocked with 10% goat serum in PBS and incubated at 37°C for 1 hour. Cells were incubated overnight with *cis* P-tau antibody (diluted in PBS and blocking serum). After washing 3 times with PBS-Tween, the cells were incubated with Alexa Fluor 488 or 546 secondary antibodies at 37°C for 1 hour. Signal detection was carried out with immunofluorescence microscopy.

For brain samples isolation, diabetic mice were perfused with PBS with 4% paraformaldehyde. Serial 8 um sections from perfused brains were collected on slides for

immunostaining analysis later. The slides were boiled on citrate buffer (pH=6) for antigen enhancement. Boiled slides were permeabilized with TritonX 0.5% at room temperature. After blocking, the slides were incubated with primary antibodies at 4°C overnight. For signal detection slides were incubated with Alexa Fluor 488 or 546 secondary antibodies. Immunostaining results for different brain areas including the brainstem cortex and hippocampus (the naming of different brain areas was according to the Allen mouse brain atlas) were quantified with ImageJ software.

Protein extraction

For protein extraction, the mouse brains were immediately removed after being snap-frozen in liquid nitrogen. These were kept at -80^{c} until they were processed. 5 mg of brain tissue was homogenized with a 300 ml lysis buffer that included protease and phosphatase inhibitors for 15 min using a mechanical homogenizer. Homogenized samples were centrifuged at 12000 g at 4°C for 20 min. The supernatant was collected and protein concentration was measured with the bicinchoninic acid assay (QIAGEN, 37901).

Immunoblotting

For western blot and SDS page analysis, 20 µg proteins were analyzed. The protein extracts from brain tissues were separated by 12% polyacrylamide gel and then transferred to PVDF membrane. Non-specific sites were blocked with 2% milk for 1 hour at room temperature. After blocking, the membranes were incubated with Pin1, oxidized Pin1, *cis* P-tau, glut3, AT180 and AT8 antibodies in 1% milk and TBS-Tween for overnight at 4°C. For signal detection membranes were incubated with HRP-conjugated secondary antibody in 1% milk and TBS-Tween for 1 hour at room temperature. Signals were visualized with the UVITEC Cambridge imaging system. Specific immunoreactive bands were quantified with ImageJ.

Malondialdehyde (MDA) assay

We studied lipid peroxidation in the brainstem and cortex employing MDA assay kit according to the manufacturer (Teb Pazhouhan Razi, Tehran, IRAN). We added butylated hydroxytoluene to the tissue homogenates to prevent peroxidation. We then added sodium dodecyl sulfate and a chromogenic solution containing thiobarbituric acid to the supernatant. The sample was subsequently subjected to spectrophotometry at 532 nm. MDA amounts in brainstem and cortex of healthy and diabetic mice were expressed as μmol /total protein.

Superoxide dismutase (SOD) activity assay

SOD enzyme activity in the brainstem and cortex of the healthy and diabetic mice were measured by SOD assay kit according to the manufacturer (Teb Pazhouhan Razi (TPR), Tehran, IRAN). Chromogenic reagent and SOD assay buffer were added to the homogenate. Sample absorbance was measured at 450 nm. The SOD enzyme activity was expressed as U/total protein.

Catalase (CAT) activity assay

CAT enzyme activity was measured by CAT assay kit according to the manufacturer (Teb Pazhouhan Razi (TPR), Tehran, IRAN). Briefly, H_2O_2, and phosphate buffer were added to the samples. Samples absorbance was measured at 540 nm. CAT enzyme activity was expressed as U/total protein.

Elevated plus-maze

Elevated plus-maze was used to assess depression-like behaviors. The elevated plus-maze has two open and closed arms that were located opposite of each other. The height of the apparatus was 100 cm above the floor. Mice were kept at the experiment room for 1h before the start of the experiment. The maze was cleaned before and between tests with 70% ethanol. Mice were placed in the center of the maze faced to one closed arm. For each mouse, the video was recorded during 5 min of free exploration. Heatmap data was collected with

python. Duration of time passed in open arms, close arms and open arm entries were calculated to assess depression-like behaviors.

Bioinformatics analysis

Differentially expressed genes (DEGs) were identified by edgeR package. We used the custom R program for visualization and data analysis. The pairwise correlation heatmaps for samples were generated based on Pearson Correlation Coefficients (PCC) using R software. The GO and pathway analysis of DEGs were performed using enrichR. The gene expression profile of the GSE78521 was obtained from a published study [30]. The significant genes were selected based on an absolute log2-fold above 1 change and FDR below 0.05 thresholds for differential expression analysis between positive (GABAergic neurons) and negative samples (other neurons)

Statistical analysis

All data were represented as mean $\pm$ SD by two-tailed unpaired Student's t test, one-way ANOVA and two-way ANOVA analyses and with 95% confidence interval. The significance level was $*P<0.05$, $**P<0.01$, $***P<0.001$, $****P<0.0001$. All significance was shown as $p<0.05$. All graphs have been created by GraphPad Prism version 6.

Results

Hyperglycemia induced tau pathology, resulting in neurodegeneration

We employed *cis* P-tau as an early driver of the tau pathogenicity process. In order to determine if hyperglycemia associated with DM, can induce *cis* P-tau accumulation, we treated primary culture neurons with different concentrations of DG (Supplementary Fig.1) and 2DG (50 mM) for the indicated periods of time (Fig. 1A). While no significant *cis* P-tau accumulation was detected in DG-treated neurons (Supplementary Figs. 1A, B), prominent

cis P-tau (Figs. 1B, C) as well as neurodegeneration were induced in those 2DG-treated neurons in a time-dependent manner (Figs. 1D, E). It is evident that DG participates in glycolysis, but not 2DG. Thus, 2DG was employed as a stress inducer. We next treated the stressed-out neurons with *cis* P-tau monoclonal antibody for 72 hours and found that the antibody can eliminate *cis* P-tau and suppress neurodegeneration in the neurons (Figs. 1B-E).

Prominent *cis* P-tau was detected in the brainstem and corpus callosum of the diabetic mouse brain

T1D mouse models were generated using Alloxan injection. The T1D modeling was confirmed with measurement of body weight, FBS, and IP-GTT (Supplementary Fig.2). The T1D mice showed significant weight loss as well as elevated FBS compared to the healthy animals (Supplementary Figs. 2A-B). Moreover, IP-GTT results showed that while healthy mice efficiently cleared the elevated serum blood glucose, the T1D mouse model had an impaired clearance of serum blood glucose (Supplementary Figs. 2C-D).

Immunofluorescence staining results showed that hyperglycemia markedly induced *cis* P-tau in diabetic mouse models in a time dependent manner (Figs. 2A-B). We showed that hyperglycemia induced profound *cis* P-tau formation in the brainstem and corpus callosum, but not in cortex and hippocampus at 96 hours post Alloxan injection (Figs. 2C-E). As mentioned above, Pin1 is responsible for converting *cis* to *trans* P-tau and its inhibition by oxidation at Cys 113 results in *cis* P-tau accumulation and neurodegeneration. We found that Pin1 was downregulated, and oxidized in the brainstem, which inversely correlated to significant accumulation of *cis* P-tau in the brainstem of those diabetic mouse models. However, this did not occur in the cortex of either healthy or the diabetic mice (Figs. 2F-G). These data suggest that Pin1 down-regulation in DM could be a potential *cis* P-tau inducer.

***Cis* p-tau spreads to various brain areas**

It has been demonstrated that *cis* P-tau is a monomeric P-tau species and has a prion nature [27]. As mentioned above, we initially observed *cis* P-tau in the brainstem and corpus callosum of DM mouse models. However, additional analysis showed that *cis* P-tau accumulation could spread to neighboring brain areas such as cortex after two months of T1D induction (Figs. 3A-B). Furthermore, we also examined other P-tau species such as AT180 using immunofluorescence staining (Fig. 3C). We found that AT180 signal was limited to the *cis* P-tau positive areas, including the brainstem at 96 hours (Fig. 3C-E). Importantly, we observed no obvious AT8 (an early tangle marker) staining in the cortex or brainstem 96 hours of the Alloxan injection (Figs. 3D-E). However, we found prominent AT8 in the cortex and brainstem at 60 days of T1D induction (Fig. 3D-E). Together, these data demonstrate that *cis* P-tau initiated tau pathology process in the DM brains; eventually leading to the spread of tau tangles formation.

Cis P-tau accumulation in GABAergic and Glutamatergic neurons led to anxiety and depression

In order to clarify the neuron subtypes of *cis* P-tau positive cells, we further examined co-localization of *cis* P-tau with various markers such as: Cholinergic (CHAT), Dopaminergic (TH), GABAergic (GAD65/67) and Glutamatergic (VGLUT1).

We found *cis* P-tau co-localized with GABAergic and Glutamatergic neurons (Figs. 4A-B). Imbalanced GABAergic & Glutamatergic neurotransmitter secretions have been reported in diabetic conditions, which can result in a depression-like behavior in the patients [31]. Thus, we examined if accumulated *cis* P-tau in these two neuron subtypes may cause depression-like behaviors in T1D model mice. In this regard, we studied the animal models behavior by employing an elevated plus maze. We observed an abnormal anxiety as well as depression-like behaviors in the T1 diabetic mouse models (Fig. 4C). Our findings are consistent with the cognitive declines observed in the DM patients.

Cis P-tau positive neurons associated expression of insulin receptors and glucose transporters

It has been reported that various Gluts and insulin receptors (IRs) are distributed unevenly in the CNS [21]. Therefore, we examined RNA sequencing data (GEO accession # GSE78521) to further address hyperglycemia-induced *cis* P-tau localization in GABAergic and Glutamatergic neurons. Our analysis revealed that Glut3 is a prominent glucose transporter in GABAergic neurons (Fig. 5A), whereas Glut 2, Glut 4 and IRs were undetectable in the *cis* P-tau positive neurons (Fig. 5B). The result demonstrates that hyperglycemia-induced *cis* P-tau response is irrespective of the aforementioned Gluts and IRs. Moreover, we observed a down-regulated Glut3 in the brainstem of the DM model mice (Fig. 5C-D)**,** suggesting that glucose supply to the neurons has been disrupted, reflecting tau pathology.

P38 inhibition suppressed *cis* P-tau formation in brain of DM mouse

We employed RNA sequencing data (GEO accession # GSE78521) to clearly demonstrate why tau pathology was observed in particular neuronal subtypes. Our bioinformatics analysis revealed that GABAergic neurons have up and down-regulated 1033 and 1004 DEGs, such as MAPK14 (P38), AKT2 and Caspase 3, compared to other neurons (Supplementary Fig.3A), (Fig. 6A). Pathway Enrichment analysis using Enrichr web tool showed that most of the DEGs are associated with advanced glycation end products (AGE) and their receptors (RAGE) signaling pathways in complications from diabetes (Fig.6B and Supplementary Fig.3B). Given that P38 as a major tau kinase is highly expressed in GABAergic neurons, we hypothesized that it may participate in the DM-induced tau pathogenicity process. Thus, we employed P38 inhibitor to examine *cis* P-tau formation in DM. We found that IP administration of SB efficiently suppressed *cis* P-tau accumulation in the DM model mice (Figs. 6C-F). Moreover, we observed a significant improvement in anxiety and depression-like behaviors in those SB treated DM mice, which was confirmed by elevated plus maze test

(Fig. 6G). It has been reported that DM may induce oxidative stress in the brain, resulting in the activation of various tau kinases [11]. Based on our aforementioned results, we further hypothesized that DM-induce oxidative stress activate tau kinases in particular brain areas. Thus, we examined SOD and CAT activities as well as MDA levels in the brainstem and cortex of diabetic mice after 96 hours of DM induction. Brainstem and cortex were used as *cis* P-tau positive and negative areas, respectively. SOD activity was found significantly higher in diabetic mice compared to the healthy group in the brainstem areas (Fig. 6H). Importantly, there were no significant difference in CAT activity and levels of MDA in the brainstem and cortex of the diabetic animals in compare to healthy controls (Figs. 6I-J). Taking these results together, we concluded that the DM conditions induce oxidative stress in the brainstem but not in the cortex of the DM mouse models.

Discussion

DM can affect the CNS and leads to comprehensive neurodegeneration. There are multiple studies showing that DM can induce tau protein hyperphosphorylation and aggregation in both T1 and T2D mouse models [19, 32, 33]. Hyperglycemia may induce tau protein hyperphosphorylation at different motifs, such as Ser202/Thr205, Ser396/Ser404, and Thr231 in T1D mice [19]. Furthermore, long-lasting hyperglycemia can induce tau hyperphosphorylation at different sites, such as Ser396/Ser404, and Thr231, resulting in cognitive decline [32]. T2DM can also induce tau hyperphosphorylation in the mouse models [33]. We demonstrated that cultured neurons under hyperglycemic conditions as well as T1DM mouse models exhibited profound tau pathology. It has been previously reported that tau pathology can spread to adjacent neurons and different brain areas [34, 35]. *Cis* P-tau has been considered as an early driver of neurodegeneration process as it shows a prion-like nature and spread in brains of TBI [27, 28]. Its role in neurodegeneration is further

highlighted by studies showing that *cis* P-tau elimination from TBI mouse models inhibits neurodegeneration while also improving learning and memory [27]. Our results showed that *cis* P-tau elimination using the respective monoclonal antibody from the hyperglycemic neurons can suppress *cis* P-tau accumulation and rescue neurodegeneration. Importantly, *cis* P-tau gradually spread to other brain areas, such as cortex two months after injection. Additionally, we found pretangle P-tau species (AT8 & AT180) 60 days after diabetes induction in the brainstem and cortex. We concluded that *cis* P-tau triggered tau pathology; resulting in tau hyperphosphorylation and tangle formation; as we previously hypothesized [21].

It is clear that metabolic stress in T2D mouse models impairs cortical and striatal GABAergic neurons, resulting in neurodegeneration in those brain areas [36]. It has also been reported that hypoglycemia can impair Glutamatergic neurons in the CNS [37], resulting in depression like behaviors [31, 38, 39]. Interestingly, we also observed depression-like behaviors in DM animal models, which is consistent with our initial observation of tau pathology in GABAergic and Glutamatergic neurons.

Impaired insulin signaling pathway or glucose metabolism deregulation can induce neuronal damage [21]. However, we did not observe IR or Glut 2 & 4 in GABAergic and Glutamatergic neurons in the brainstem. Therefore, we concluded that the stress responses were irrespective to the IRs or those Gluts. On the other hand, Glut3 is a major neuronal glucose transporter in GABAergic neurons and can be decreased in a DM brain [40, 41]. A prominent decrease in Glut3 expression level in DM mice may contribute to the compromised brain energy metabolism during metabolic diseases; such as DM.

Diabetes can modify the functionality of antioxidant enzymes in the brain; reflecting oxidative stress [42, 43]. It has been reported that SOD and CAT activities are increased in early diabetic rat models (72 hours). However, CAT, but not SOD activity, increases in long

term diabetes [44]. We showed an increase in SOD activity in the brainstem of diabetic mouse model resulted in increased superoxide radical production, at 96 hours after Alloxan injection. The oxidative stress triggers several pathogenic cascades, resulting in tau pathology. Consistent with previous findings [11, 45], stress activated P38 (particularly the α-isoform) in turn phosphorylated tau, Our bioinformatics analysis showed that although GABAergic neurons highly express P38, we could not detect a significant difference between the brainstem and other brain areas. This was likely due to the scattered distribution of different neuron types. Importantly, P38 inhibition rescued tau pathology and alleviated depression-like behaviors in the DM mouse brain. On the other hand, we found Pin1, the isomerase responsible for *cis* to *trans* conversion, was down-regulated along with its oxidation in the *cis* P-tau positive brain areas of DM mouse models, which is consistent with its role in facilitating *cis* P-tau accumulation [25, 27]. Our data suggest that the oxidative stress causes Pin1 oxidation, which is reflected by *cis* P-tau accumulation, and that both DM-induced P38 activation and Pin1 suppression contribute to oxidative stress induced tau pathology.

Conclusion

Tau pathology and neurodegeneration have been clearly observed in the DM brain. However, it has remained elusive as to how DM conditions reflect neurodegeneration. We demonstrated that DM conditions trigger oxidative stress in the glutamatergic and GABAergic neurons in the brainstem, which in turn activate P38 and suppress Pin1; both resulting in pathogenic *cis* P-tau accumulation. Pathogenic tau eventually spreads to other brain areas resulting in a comprehensive tau hyperphosphorylation and aggregation in the DM brain.

Abbreviations

CAT (catalase), DEGs (differentially expressed genes), DG (D-glucose), 2DG (2-Deoxy-D-glucose), DM (diabetes mellitus), FBS (fasting blood glucose), FDA (Fluorescein diacetate), Gluts (glucose transporters), IRs (insulin receptors), IP (intraperitoneal), IP-GTT (IP glucose tolerance test), MDA (malondialdehyde), PCC (Pearson Correlation Coefficients), PI (Propidium Iodide), SB (SB203580), SOD (superoxide dismutase), T1D, T2D (type 1 or 2 diabetes), TBI (traumatic brain injury).

Acknowledgement

We would like to express our deepest thanks to Prof. Kun Ping Lu for his generosity on supplying conformation-specific anti-tau and anti oxi-Pin1 antibodies.

Funding

This study has been supported by grant #97014846 from Iran National Science Foundation.

Availability of data and materials

All data generated or analyzed during this study are included in this published article [and its supplementary information files].

Authors' contributions

A Farhadi: performed the experiments, analyzed the data and wrote the paper. F Hadi, M Totonchi, A Mousavi, SM Nabavi, H Baharvand, H Pakdaman, EH Saffar, H Al-Sinawi, Q Li: performed the experiments and analyzed the data. JS Zhang, Y Tahamtani, and K Shahpasand: designed the study, analyzed the data and wrote the paper. All authors read and approved the final manuscript.

Ethics approval and consent to participate

Animal experiments were approved by Institutional Animal Care and Use Committee.

Competing interests

Authors declare that there is no conflict of interest.

References

.1 Saberzadeh-Ardestani B, Karamzadeh R, Basiri M, Hajizadeh-Saffar E, Farhadi A, Shapiro AMJ, Tahamtani Y, Baharvand H: **Type 1 Diabetes Mellitus: Cellular and Molecular Pathophysiology at A Glance.** *Cell J* 2018, **20:**294-301.

.2 Huang CC, Chung CM, Leu HB ,Lin LY, Chiu CC, Hsu CY, Chiang CH, Huang PH, Chen TJ, Lin SJ, et al: **Diabetes mellitus and the risk of Alzheimer's disease: a nationwide population-based study.** *PLoS One* 2014, **9:**e87095.

.3 Chatterjee S, Peters SA, Woodward M, Mejia Arango S, Batty GD, Beckett N, Beiser A, Borenstein AR, Crane PK, Haan M, et al: **Type 2 Diabetes as a Risk Factor for Dementia in Women Compared With Men: A Pooled Analysis of 2.3 Million People Comprising More Than 100,000 Cases of Dementia.** *Diabetes Care* 2016, **39:**300-307.

.4 Fan YC, Hsu JL, Tung HY, Chou CC, Bai CH: **Increased dementia risk predominantly in diabetes mellitus rather than in hypertension or hyperlipidemia: a population-based cohort study.** *Alzheimers Res Ther* 2017, **9:**7.

.5 Kuo CL, Lu CL, Chang YH, Li CY: **Population-Based Cohort Study on Dementia Risk in Patients with Type 1 Diabetes Mellitus.** *Neuroepidemiology* 2018, **50:**57-62.

.6 Schmidt R, Launer LJ, Nilsson LG, Pajak A, Sans S, Berger K, Breteler MM, de Ridder M, Dufouil C, Fuhrer R, et al: **Magnetic resonance imaging of the brain in diabetes: the Cardiovascular Determinants of Dementia (CASCADE) Study.** *Diabetes* 2004, **53:**687-692.

.7 Moran C, Beare R, Phan TG, Bruce DG, Callisaya ML, Srikanth V: **Type 2 diabetes mellitus and biomarkers of neurodegeneration.** *Neurology* 2015, **85:**1123-1130.

.8 Marseglia A, Fratiglioni L, Kalpouzos G, Wang R, Backman L, Xu W: **Prediabetes and diabetes accelerate cognitive decline and predict microvascular lesions: A population-based cohort study.** *Alzheimers Dement* 2019, **15:**25-33.

.9 Elahi M, Hasan Z, Motoi Y, Matsumoto SE, Ishiguro K, Hattori N: **Region-Specific Vulnerability to Oxidative Stress, Neuroinflammation, and Tau Hyperphosphorylation in Experimental Diabetes Mellitus Mice.** *J Alzheimers Dis* 2016, **51:**1209-1224.

.10 Qu Z, Jiao Z ,Sun X, Zhao Y, Ren J, Xu G: **Effects of streptozotocin-induced diabetes on tau phosphorylation in the rat brain.** *Brain Res* 2011, **1383:**300-306.

.11 Sharma R, Buras E, Terashima T, Serrano F, Massaad CA, Hu L, Bitner B, Inoue T, Chan L, Pautler RG: **Hyperglycemia induces oxidative stress and impairs axonal transport rates in mice.** *PLoS One* 2010, **5:**e13463.

.12 Ouwens DM, van Duinkerken E, Schoonenboom SN, Herzfeld de Wiza D, Klein M, van Golen L, Pouwels PJ, Barkhof F, Moll AC, Snoek FJ, et al: **Cerebrospinal fluid levels of Alzheimer's disease biomarkers in middle-aged patients with type 1 diabetes.** *Diabetologia* 2014, **57:**2208-2214.

.13 Clodfelder-Miller BJ, Zmijewska AA, Johnson GV, Jope RS: **Tau is hyperphosphorylated at multiple sites in mouse brain in vivo after streptozotocin-induced insulin deficiency.** *Diabetes* 2006, **55:**3320-3325.

.14 Jolivalt CG, Lee CA, Beiswenger KK, Smith JL, Orlov M, Torrance MA, Masliah E: **Defective insulin signaling pathway and increased glycogen synthase kinase-3 activity in the brain of diabetic mice: parallels with Alzheimer's disease and correction by insulin.** *J Neurosci Res* 2008, **86:**3265-3274.

.15 Fitzpatrick AWP, Falcon B, He S, Murzin AG, Murshudov G, Garringer HJ, Crowther RA, Ghetti B, Goedert M, Scheres SHW: **Cryo-EM structures of tau filaments from Alzheimer's disease.** *Nature* 2017, **547:**185-190.

.16 Hadi F, Akrami H, Shahpasand K, Fattahi MR: **Wnt signalling pathway and tau phosphorylation: A comprehensive study on known connections.** *Cell Biochem Funct* 2020.

.17 Manassero G ,Guglielmotto M, Monteleone D, Vasciaveo V, Butenko O, Tamagno E, Arancio O, Tabaton M: **Dual Mechanism of Toxicity for Extracellular Injection of Tau Oligomers versus Monomers in Human Tau Mice.** *J Alzheimers Dis* 2017, **59:**743-751.

.18 Kellogg EH, Hejab NMA ,Poepsel S, Downing KH, DiMaio F, Nogales E: **Near-atomic model of microtubule-tau interactions.** *Science* 2018, **360:**1242-1246.

.19 Gratuze M, Julien J, Petry FR, Morin F, Planel E: **Insulin deprivation induces PP2A inhibition and tau hyperphosphorylation in hTau mice, a model of Alzheimer's disease-like tau pathology.** *Sci Rep* 2017, **7:**46359.

.20 Lauretti E, Pratico D: **Glucose deprivation increases tau phosphorylation via P38 mitogen-activated protein kinase.** *Aging Cell* 2015, **14:**1067-1074.

.21 Farhadi A, Vosough M, Zhang JS, Tahamtani Y, Shahpasand K: **A Possible Neurodegeneration Mechanism Triggered by Diabetes.** *Trends Endocrinol Metab* 2019, **30:**692-700.

.22 Lauretti E, Li JG, Di Meco A, Pratico D: **Glucose deficit triggers tau pathology and synaptic dysfunction in a tauopathy mouse model.** *Transl Psychiatry* 2017, **7:**e1020.

.23 Maphis N, Jiang S, Xu G, Kokiko-Cochran ON, Roy SM, Van Eldik LJ, Watterson DM, Lamb BT, Bhaskar K: **Selective suppression of the alpha isoform of p38 MAPK rescues late-stage tau pathology** *.Alzheimers Res Ther* 2016, **8:**54.

.24 Nakamura K, Greenwood A, Binder L, Bigio EH, Denial S, Nicholson L, Zhou XZ, Lu KP: **Proline isomer-specific antibodies reveal the early pathogenic tau conformation in Alzheimer's disease.** *Cell* 2012, **149:**232-244.

.25 Chen CH, Li W, Sultana R, You MH, Kondo A, Shahpasand K, Kim BM, Luo ML, Nechama M, Lin YM, et al: **Pin1 cysteine-113 oxidation inhibits its catalytic activity and cellular function in Alzheimer's disease.** *Neurobiol Dis* 2015, **76:**13-23.

.26 Naserkhaki R, Zamanzadeh S, Baharvand H, Nabavi SM, Pakdaman H, Shahbazi S, Vosough M, Ghaedi G, Barzegar A, Mirtorabi D, et al: **cis pT231-Tau Drives Neurodegeneration in Bipolar Disorder.** *ACS Chem Neurosci* 2019, **10:**1214-1221.

.27 Kondo A, Shahpasand K, Mannix R, Qiu J, Moncaster J, Chen CH, Yao Y, Lin YM, Driver JA, Sun Y, et al: **Antibody against early driver of neurodegeneration cis P-tau blocks brain injury and tauopathy.** *Nature* 2015, **523:**431-436.

.28 Albayram O, Kondo A, Mannix R, Smith C, Tsai CY, Li C, Herbert MK, Qiu J, Monuteaux M, Driver J, et al: **Cis P-tau is induced in clinical and preclinical brain injury and contributes to post-injury sequelae.** *Nat Commun* 2017, **8:**1000.

.29 Jiajia L, Shinghung M, Jiacheng Z, Jialing W, Dilin X, Shengquan H, Zaijun Z, Qinwen W ,Yifan H, Wei C: **Assessment of Neuronal Viability Using Fluorescein Diacetate-Propidium Iodide Double Staining in Cerebellar Granule Neuron Culture.** *J Vis Exp* 2017.

.30 Lutas A, Lahmann C, Soumillon M, Yellen G: **The leak channel NALCN controls tonic firing and glycolytic sensitivity of substantia nigra pars reticulata neurons.** *Elife* 2016, **5**.

.31 Liu K, Zhao L, Xu W, Lin Q, Zhou Y, Huang X, Ye X, He J, Bai G, Yan Z, Gao H: **Metabolic Changes Associated with a Rat Model of Diabetic Depression Detected by Ex Vivo (1)H**

Nuclear Magnetic Resonance Spectroscopy in the Prefrontal Cortex, Hippocampus, and Hypothalamus. *Neural Plast* 2018, **2018:**6473728.

.32 Wu J, Zhou SL, Pi LH, Shi XJ, Ma LR, Chen Z, Qu ML, Li X, Nie SD, Liao DF, et al: **High glucose induces formation of tau hyperphosphorylation via Cav-1-mTOR pathway: A potential molecular mechanism for diabetes-induced cognitive dysfunction.** *Oncotarget* 2017, **8:**40843-40856.

.33 Kim B, Backus C, Oh S, Hayes JM, Feldman EL: **Increased tau phosphorylation and cleavage in mouse models of type 1 and type 2 diabetes.** *Endocrinology* 2009, **150:**5294-5301.

.34 Wegmann S, Bennett RE, Delorme L, Robbins AB, Hu M, McKenzie D, Kirk MJ, Schiantarelli J, Tunio N, Amaral AC, et al: **Experimental evidence for the age dependence of tau protein spread in the brain.** *Sci Adv* 2019, **5:**eaaw6404.

.35 Scialo C, De Cecco E, Manganotti P, Legname G: **Prion and Prion-Like Protein Strains: Deciphering the Molecular Basis of Heterogeneity in Neurodegeneration.** *Viruses* 2019, **11**.

.36 Larsson M, Lietzau G ,Nathanson D, Ostenson CG, Mallard C, Johansson ME, Nystrom T, Patrone C, Darsalia V: **Diabetes negatively affects cortical and striatal GABAergic neurons: an effect that is partially counteracted by exendin-4.** *Biosci Rep* 2016, **36**.

.37 Chowdhury GMI, Wang P, Ciardi A, Mamillapalli R, Johnson J, Zhu W, Eid T, Behar K, Chan O: **Impaired Glutamatergic Neurotransmission in the Ventromedial Hypothalamus May Contribute to Defective Counterregulation in Recurrently Hypoglycemic Rats.** *Diabetes* 2017, **66:**1979-1989.

.38 Zheng Y, Yang Y, Dong B, Zheng H, Lin X, Du Y, Li X, Zhao L, Gao H: **Metabonomic profiles delineate potential role of glutamate-glutamine cycle in db/db mice with diabetes-associated cognitive decline.** *Mol Brain* 2016, **9:**40.

.39 Ajilore O, Haroon E, Kumaran S, Darwin C, Binesh N, Mintz J, Miller J, Thomas MA, Kumar A: **Measurement of brain metabolites in patients with type 2 diabetes and major depression using proton magnetic resonance spectroscopy.** *Neuropsychopharmacology* 2007, **32:**1224-1231.

.40 Liu Y ,Liu F, Grundke-Iqbal I, Iqbal K, Gong CX: **Brain glucose transporters, O-GlcNAcylation and phosphorylation of tau in diabetes and Alzheimer's disease.** *J Neurochem* 2009, **111:**242-249.

.41 Mergenthaler P, Lindauer U, Dienel GA, Meisel A: **Sugar for the brain** :**the role of glucose in physiological and pathological brain function.** *Trends Neurosci* 2013, **36:**587-597.

.42 Szaleczky E, Prechl J, Feher J, Somogyi A: **Alterations in enzymatic antioxidant defence in diabetes mellitus--a rational approach.** *Postgrad Med J* 1.17 75:13 ,999

.43 Ceretta LB, Reus GZ, Abelaira HM, Ribeiro KF, Zappellini G, Felisbino FF, Steckert AV, Dal-Pizzol F, Quevedo J: **Increased oxidative stress and imbalance in antioxidant enzymes in the brains of alloxan-induced diabetic rats.** *Exp Diabetes Res* 2012, **2012:**302682.

.44 Ramanathan M, Jaiswal AK, Bhattacharya SK: **Superoxide dismutase, catalase and glutathione peroxidase activities in the brain of streptozotocin induced diabetic rats.** *Indian J Exp Biol* 1999, **37:**182-183.

.45 Sun Y, Xiao Q, Luo C ,Zhao Y, Pu D, Zhao K, Chen J, Wang M, Liao Z: **High-glucose induces tau hyperphosphorylation through activation of TLR9-P38MAPK pathway.** *Exp Cell Res* 2017, **359:**312-318.

Figure legends

Fig. 1 Accumulation of pathogenic *cis* P-tau cultured neurons in hyperglycemic conditions. (**A**) Schematic representation of primary culture neurons generated from embryonic mouse brain. (**B**) Immunostained primary neurons with *cis* P-tau mAb, cultured under hyperglycemic conditions for 72 hours. The stress profoundly induced *cis* P-tau in the neurons. Treatment of neurons with *cis* P-tau monoclonal antibody significantly decreased *cis* P-tau formation. (**C**) Quantification of immunostained neurons in section B, *p <0.05, ***p < 0.001. (**D**) Live and dead cell assay of neurons cultured in hyperglycemic conditions at different time points. Percentage of live cells was significantly decreased after 72 hours in cultured neurons under hyperglycemic conditions. While hyperglycemia induced neurodegeneration, optional *cis* P-tau removal suppressed the neuronal cell death. Green: live; red: dead. (**E**) Quantification of section D, ***p < 0.001, ****p < 0.0001. Data represented as mean ± SD. D: day, G: group, A-*cis*: Anti-*cis* monoclonal antibody, -7D: expansion for 7 days.

Fig. 2 Hyperglycemia induces *cis* P-tau in specific brain areas of model mouse in a time dependent manner. (**A**) Immunostained mouse brain tissues with *cis* P-tau mAb at indicated time points. Results showed significant *cis* P-tau staining in diabetic mouse brain after 96 hours of stress induction. (**B**) Quantification analysis of part A, *p <0.05, **p < 0.01, ***P<0.001. (**C-D**) Various brain areas of diabetic mice stained with *cis* P-tau mAb. Note the prominent *cis* P-tau accumulations in the brainstem and corpus callosum of the DM mice compared to the healthy control, whereas no to minimal amount of *cis* P-tau was detected in the cortex or hippocampus of either DM or healthy control. (**E**) Quantification of immunoblot images in section C, ****P<0.0001. (**F**) Immunoblot analysis of diabetic and healthy mice stained with Pin1, oxidized Pin1, and *cis* P-tau. *Cis* P-tau was significantly increased,

whereas Pin1 was downregulated and oxidized under diabetic conditions in the brainstem of diabetic mouse. (**G**) Quantification of immunoblots in section F, *P<0.05, ****P<0.0001. The data are presented as mean ± SD. BS: brainstem, CC: corpus callosum, COR: cortex, HPC: hippocampus. ND: not detectable.

Fig.3 DM induces prominent tau phosphorylation and *cis* P-tau spreading. (**A**) Immunofluorescence staining of brain tissue from DM mice showed *cis* P-tau spread and *cis* P-tau accumulation in the other parts of the brain including cortex 60 days of stress treatment. There was no significant difference of *cis* P-tau levels in hippocampus over 60 days of stress treatment. (**B**) Quantification of part A, ****P<0.0001. (**C**) Different brain areas were stained with AT180 antibody after 96 hours and 60 days. There was prominent AT180 staining in *cis* P-tau positive areas, including the brainstem, after 96 hours. After 60 days, AT180 was detected in the brainstem and cortex of DM mouse models. (**D**) Immunoblot analysis of DM mouse models brain stained with AT180 and AT8. AT180 was prominent in brainstem after 96 hours and increased in the cortex and brainstem after 60 days. AT8 formation was increased significantly after 60 days. There was no prominent AT8 in brainstem and cortex of DM mouse models after 96 hours. (**E**) Quantification representation of part D, *p <0.05, **p < 0.01. Data represented as mean ± SD. D: days, h: hours. ns: not significant.

Fig. 4 Pathogenic *cis* P-tau colocalizes with specific neurons in diabetic mouse brainstem, resulting in depressive like behaviors. (**A**) Immunostained DM mouse brains with different neuron markers. *Cis* P-tau was colocalized with GABAergic (GAD65/67) and glutamatergic (Vglut1) neurons. (**B**) Quantification of section A, ****P<0.0001. (**C**) Graphs representing time spent in open or closed arms. DM mouse models showed abnormal risk-

taking behavior by spending more time in open arms than control healthy animals, *P<0.05. Data represented as mean ± SD.

Fig. 5 *Cis* P-tau positive neurons express different gluts and IRs. (**A**) Bioinformatic analysis demonstrates various mRNA expression patterns of IRs and different gluts in midbrain GABAergic neurons. (**B**) Immunostained T1D brain sections with IRs and Gluts. As demonstrated in the figure, *cis* P-tau positive neurons do not colocalize with gluts and IRs in the diabetic mouse brains. (**C**) Immunoblots of the diabetic and healthy mouse brains stained with Glut3. (**D**) Quantification of the blots in section C, *P<0.05. There was a significantly different Glut3 expression pattern in diabetic and healthy control mouse brains. Data represented as mean ± SD. COR: cortex, BS: brainstem, Slc2a2: Glut2, Slc2a3: Glut3, Slc2a4: Glut4, Insr: insulin receptor.

Fig. 6 P38 is highly expressed in midbrain GABAergic neurons. (**A**) Scatter plot analysis of expressed genes showed that MAPK14, AKT and Caspase3 are differentially expressed in midbrain GABAergic neurons compared to other neuron types. (**B**) KEGG pathway analysis showed that the AGE/RAGE signaling pathway in diabetic complications is an important pathway that is being upregulated in GABAergic neurons. (**C**) DM mouse brains stained with *cis* P-tau mAb after 96 hrs. *cis* P-tau was significantly decreased by SB daily injection. (**D**) Quantification of section C *P<0.05. *Cis* P-tau formation was significantly decreased in SB injected mice compared to the untreated diabetic group. (**E**) Immunoblot analysis of DM mouse brains stained with *cis* P-tau mAb. (**F**) Quantification of the blots in section E, *P<0.05. (**G**) Elevated plus maze analysis of SB treated or untreated DM mouse models. SB treatment profoundly suppressed depression-like behaviors of the DM animals, *P<0.05, **P<0.01. (**H**) SOD enzyme activity was significantly higher in brainstem of diabetic mice compared to the healthy group after 96 hours, *P<0.05. (**I**) CAT enzyme activity was not

significant elevated in the cortex and brainstem of diabetic mice compared to the healthy group. (**J**) MDA levels in the cortex and brainstem of diabetic mice were not higher in diabetic group compared to the healthy group. BS:brainstem, COR:cortex. Data represented as mean ± SD.

Figures

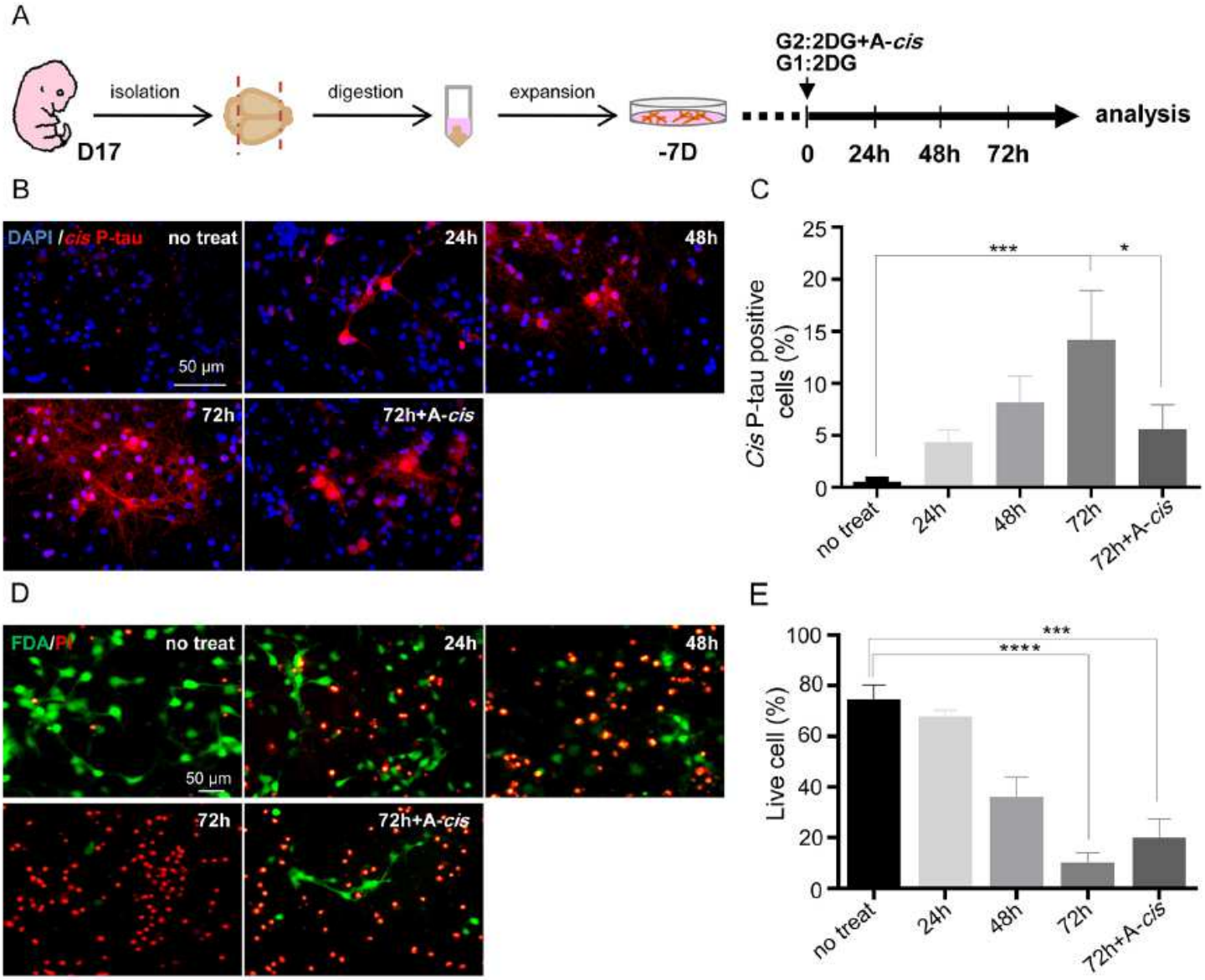

Figure 1

Accumulation of pathogenic cis P-tau cultured neurons in hyperglycemic conditions. (A) Schematic representation of primary culture neurons generated from embryonic mouse brain. (B) Immunostained primary neurons with cis P-tau mAb, cultured under hyperglycemic conditions for 72 hours. The stress profoundly induced cis P-tau in the neurons. Treatment of neurons with cis P-tau monoclonal antibody significantly decreased cis P-tau formation. (C) Quantification of immunostained neurons in section B, *p <0.05, ***p < 0.001. (D) Live and dead cell assay of neurons cultured in hyperglycemic conditions at different time points. Percentage of live cells was significantly decreased after 72 hours in cultured neurons under hyperglycemic conditions. While hyperglycemia induced neurodegeneration, optional cis P-tau removal suppressed the neuronal cell death. Green: live; red: dead. (E) Quantification of section D,

***p < 0.001, ****p < 0.0001. Data represented as mean ± SD. D: day, G: group, A-cis: Anti-cis monoclonal antibody, -7D: expansion for 7 days.

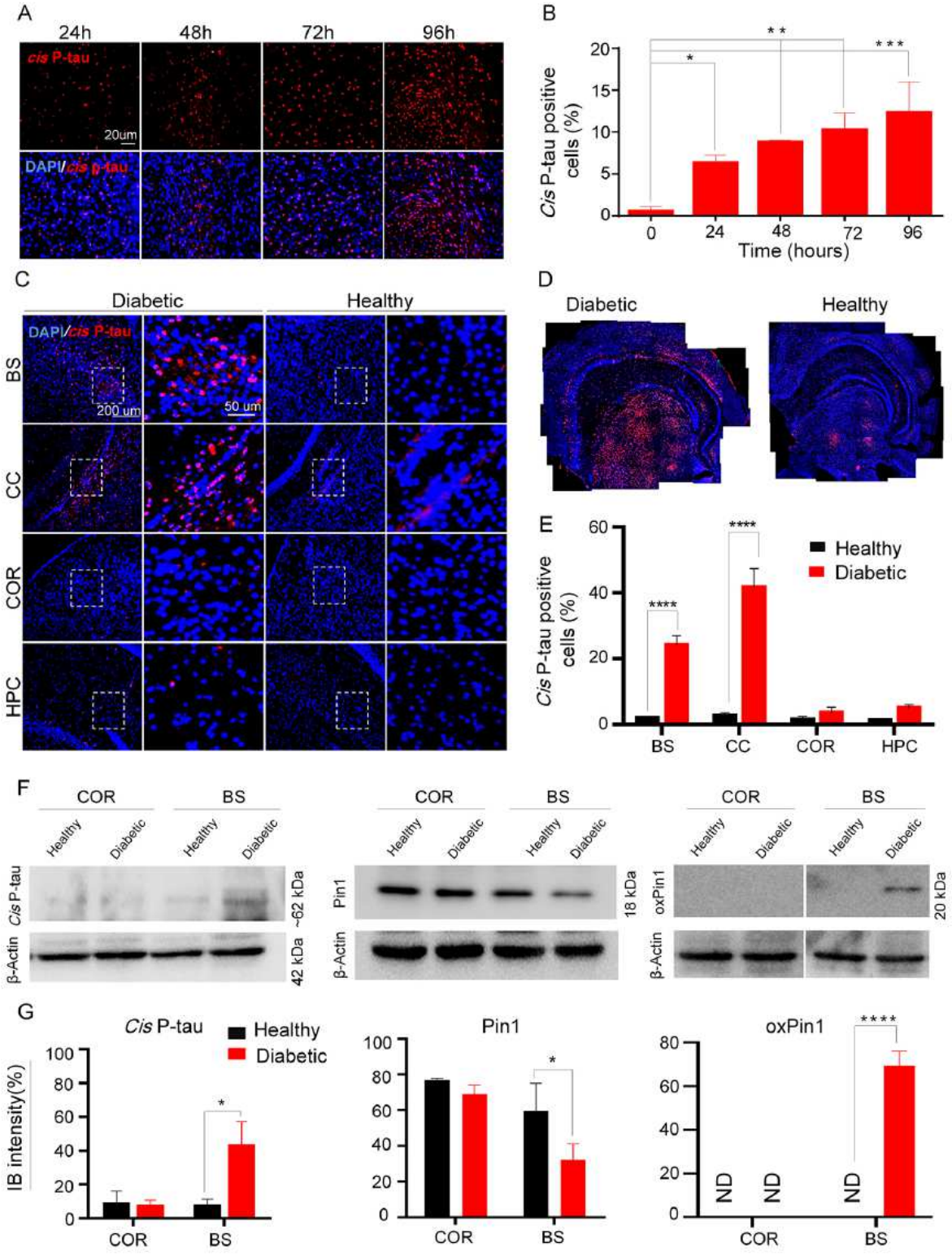

Figure 2

Hyperglycemia induces cis P-tau in specific brain areas of model mouse in a time dependent manner. (A) Immunostained mouse brain tissues with cis P-tau mAb at indicated time points. Results showed significant cis P-tau staining in diabetic mouse brain after 96 hours of stress induction. (B) Quantification

analysis of part A, *p <0.05, **p < 0.01, ***P<0.001. (C-D) Various brain areas of diabetic mice stained with cis P-tau mAb. Note the prominent cis P-tau accumulations in the brainstem and corpus callosum of the DM mice compared to the healthy control, whereas no to minimal amount of cis P-tau was detected in the cortex or hippocampus of either DM or healthy control. (E) Quantification of immunoblot images in section C, ****P<0.0001. (F) Immunoblot analysis of diabetic and healthy mice stained with Pin1, oxidized Pin1, and cis P-tau. Cis P-tau was significantly increased, whereas Pin1 was downregulated and oxidized under diabetic conditions in the brainstem of diabetic mouse. (G) Quantification of immunoblots in section F, *P<0.05, ****P<0.0001. The data are presented as mean ± SD. BS: brainstem, CC: corpus callosum, COR: cortex, HPC: hippocampus. ND: not detectable.

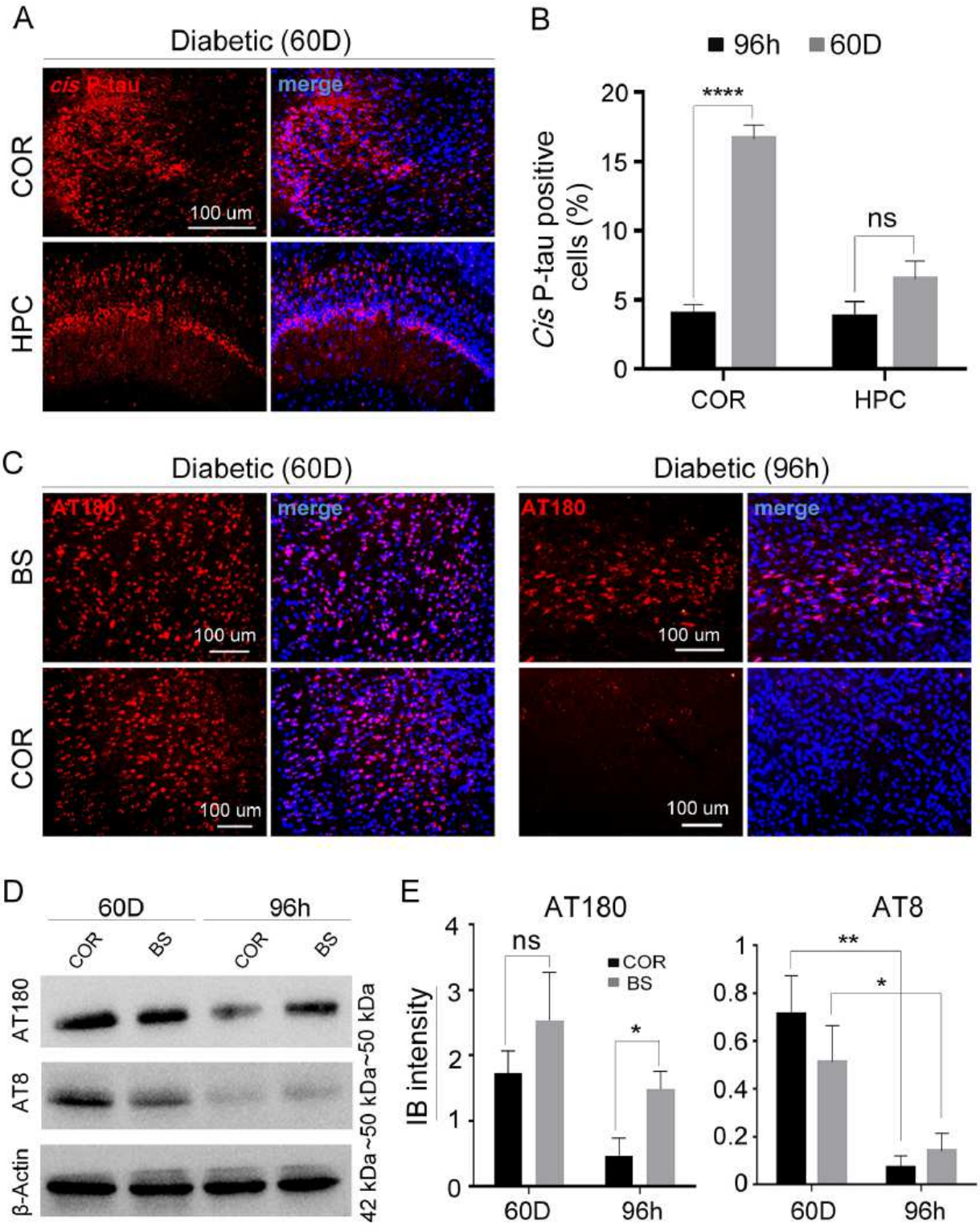

Figure 3

DM induces prominent tau phosphorylation and cis P-tau spreading. (A) Immunofluorescence staining of brain tissue from DM mice showed cis P-tau spread and cis P-tau accumulation in the other parts of the brain including cortex 60 days of stress treatment. There was no significant difference of cis P-tau levels in hippocampus over 60 days of stress treatment. (B) Quantification of part A, ****P<0.0001. (C) Different brain areas were stained with AT180 antibody after 96 hours and 60 days. There was prominent AT180

staining in cis P-tau positive areas, including the brainstem, after 96 hours. After 60 days, AT180 was detected in the brainstem and cortex of DM mouse models. (D) Immunoblot analysis of DM mouse models brain stained with AT180 and AT8. AT180 was prominent in brainstem after 96 hours and increased in the cortex and brainstem after 60 days. AT8 formation was increased significantly after 60 days. There was no prominent AT8 in brainstem and cortex of DM mouse models after 96 hours. (E) Quantification representation of part D, *p <0.05, **p < 0.01. Data represented as mean ± SD. D: days, h: hours. ns: not significant.

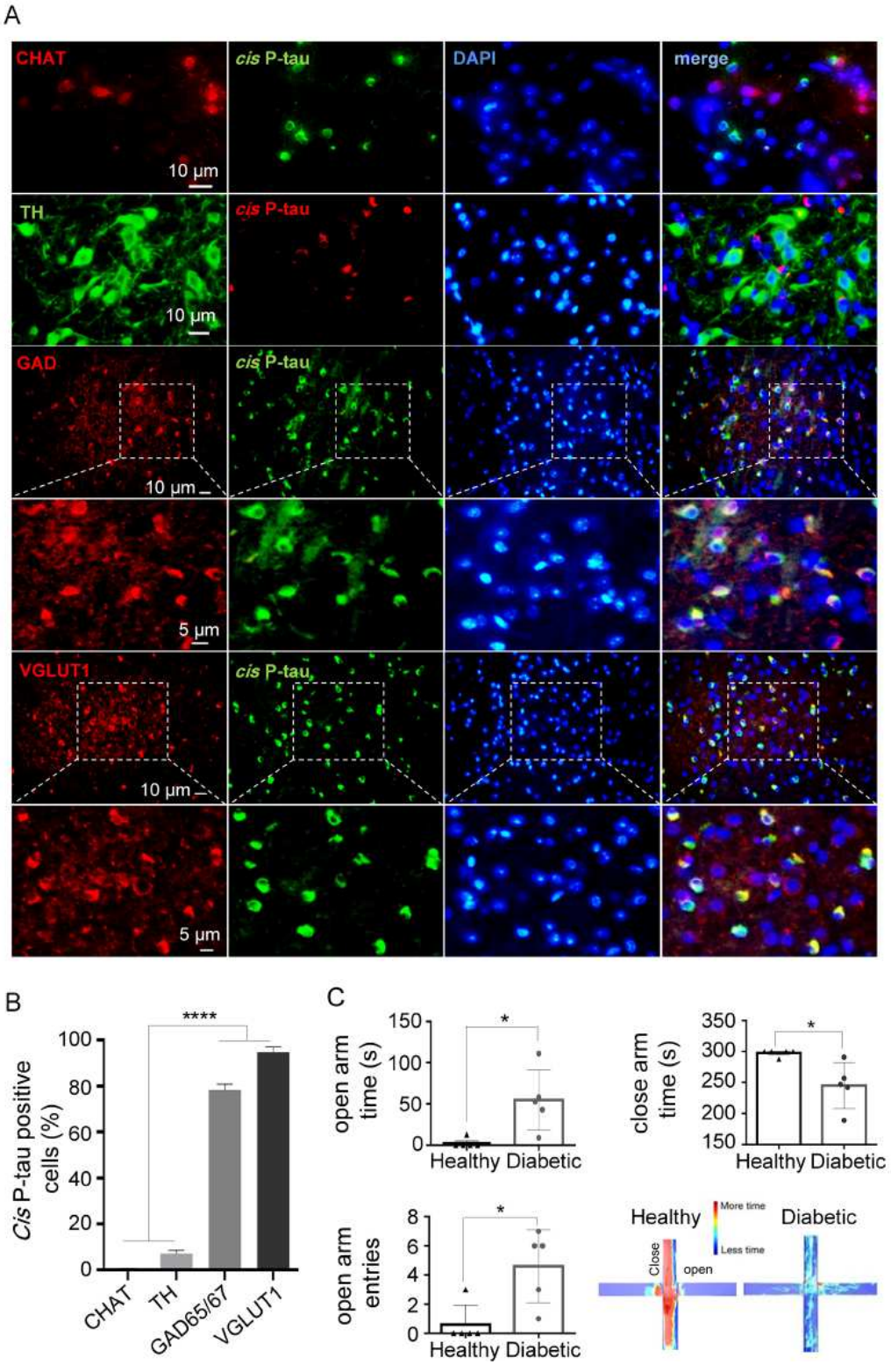

Figure 4

Pathogenic cis P-tau colocalizes with specific neurons in diabetic mouse brainstem, resulting in depressive like behaviors. (A) Immunostained DM mouse brains with different neuron markers. Cis P-tau was colocalized with GABAergic (GAD65/67) and glutamatergic (Vglut1) neurons. (B) Quantification of section A, ****P<0.0001. (C) Graphs representing time spent in open or closed arms. DM mouse models showed abnormal risk-taking behavior by spending more time in open arms than control healthy animals, *P<0.05. Data represented as mean ± SD.

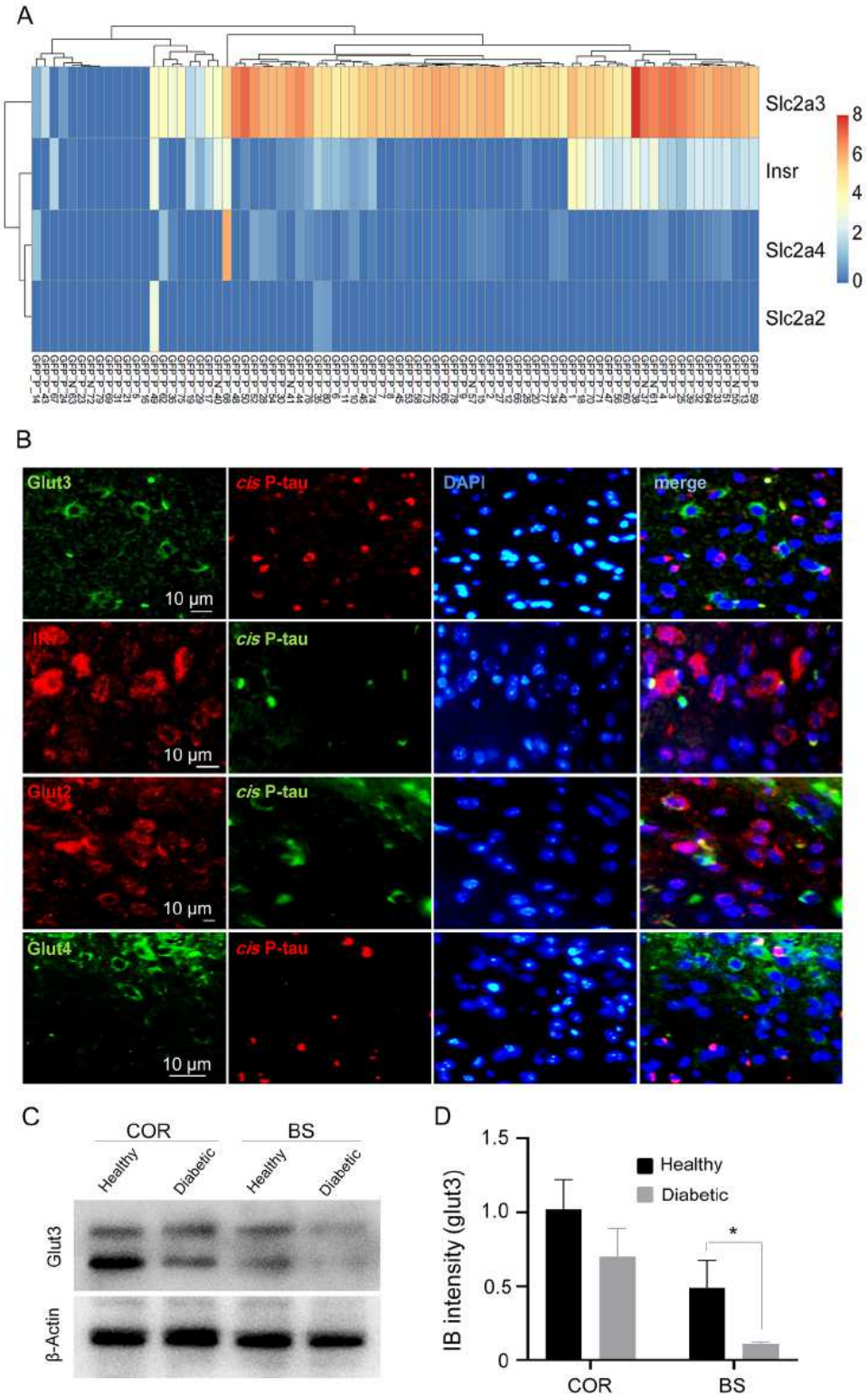

Figure 5

Cis P-tau positive neurons express different gluts and IRs. (A) Bioinformatic analysis demonstrates various mRNA expression patterns of IRs and different gluts in midbrain GABAergic neurons. (B) Immunostained T1D brain sections with IRs and Gluts. As demonstrated in the figure, cis P-tau positive neurons do not colocalize with gluts and IRs in the diabetic mouse brains. (C) Immunoblots of the diabetic and healthy mouse brains stained with Glut3. (D) Quantification of the blots in section C, *P<0.05. There was a significantly different Glut3 expression pattern in diabetic and healthy control mouse brains. Data represented as mean ± SD. COR: cortex, BS: brainstem, Slc2a2: Glut2, Slc2a3: Glut3, Slc2a4: Glut4, Insr: insulin receptor.

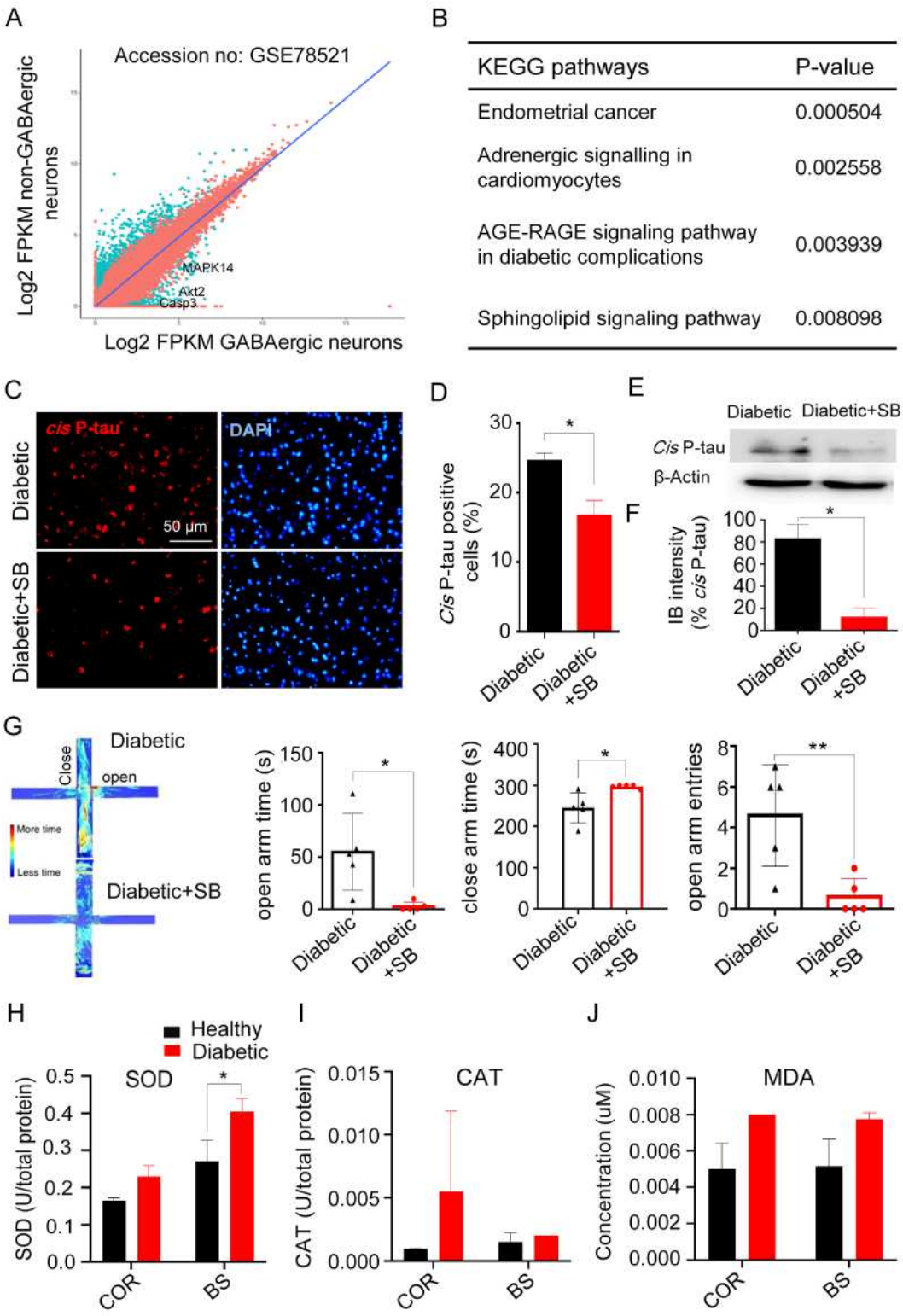

Figure 6

P38 is highly expressed in midbrain GABAergic neurons. (A) Scatter plot analysis of expressed genes showed that MAPK14, AKT and Caspase3 are differentially expressed in midbrain GABAergic neurons compared to other neuron types. (B) KEGG pathway analysis showed that the AGE/RAGE signaling pathway in diabetic complications is an important pathway that is being upregulated in GABAergic neurons. (C) DM mouse brains stained with cis P-tau mAb after 96 hrs. cis P-tau was significantly

decreased by SB daily injection. (D) Quantification of section C *P<0.05. Cis P-tau formation was significantly decreased in SB injected mice compared to the untreated diabetic group. (E) Immunoblot analysis of DM mouse brains stained with cis P-tau mAb. (F) Quantification of the blots in section E, *P<0.05. (G) Elevated plus maze analysis of SB treated or untreated DM mouse models. SB treatment profoundly suppressed depression-like behaviors of the DM animals, *P<0.05, **P<0.01. (H) SOD enzyme activity was significantly higher in brainstem of diabetic mice compared to the healthy group after 96 hours, *P<0.05. (I) CAT enzyme activity was not significant elevated in the cortex and brainstem of diabetic mice compared to the healthy group. (J) MDA levels in the cortex and brainstem of diabetic mice were not higher in diabetic group compared to the healthy group. BS:brainstem, COR:cortex. Data represented as mean ± SD.

Supplementary Files

This is a list of supplementary files associated with this preprint. Click to download.

- 630Supplinfo.pdf